Transition in wear regime during braking applications: an analysis of the debris and surfaces of the brake pad and disc

L. Y. Barros[*a], J. C. Poletto[a,b,c], G. Gehlen[a], G. Lasch[a], P. D. Neis[a], A. Ramalho[d], N. F. Ferreira[a,d]

[a]Laboratory of Tribology, Federal University of Rio Grande do Sul, Porto Alegre, Brazil
[b]Soete Laboratory, Ghent University, Ghent, Belgium
[c]Flanders Make @ Ugent – Core Lab MIRO, Ghent, Belgium
[d]CEMMPRE, ARISE, Department of Mechanical Engineering, University of Coimbra, Coimbra, Portugal

Received Date Line (to be inserted by Production) (8 pt)

Abstract

This article aims to describe the sequence of events (cause-effect) that lead to the transition in wear regime from moderate to severe for brake friction materials (BFM). Tribofilm, contact plateaus and wear debris are characterized in both regimes through different techniques. It was concluded that there is a critical tensile strength which leads to the destruction of the contact plateaus (the secondary type), resulting in a direct contact between the metallic fibers of the BFM and the tribofilm deposited on the disc's surface. Then, the tribofilm is gradually removed over the braking applications, increasing the wear rate of the tribopair.

Keywords: Brake friction materials, Wear regime, Third body, Pad's morphology

1 Introduction

In the recent literature, many studies aim to improve the quality of brake friction materials (BFM). For instance, natural and ceramic fibers [1,2], residual ingredients [3,4], carbon fibers [5] and different resins [6] are added in BFM's formulations in order to improve their friction and wear performance and/or reduce the negative impact in the environment. Thus, manufacturers of BFM have conducted numerous experiments to reach an appropriate friction level in their formulations. Reaching a stable friction behavior under a wide range of conditions (i.e., contact pressure, sliding velocity and temperature) is crucial [7,8]. In addition to friction, the wear of the BFM should be minimized during braking applications. In this regard, a clear outlook of the processes related to the transition in wear regime is key for the development of durable BFM. The transition in wear regime is a phenomenon where a sudden change in the BFM's wear rate occurs. This change is often caused by an alteration in the braking condition (for instance, an increase in the contact pressure). The transition in the wear regime (from moderate to severe) is associated with transformations in the contact conditions, as well as in the physical characteristics of the worn surfaces [9].

A great number of investigations have been made to clarify and understand the so-called third body in brake pad-disc systems. During a braking, wear debris can be trapped between the tribopair surface, forming the third body. The portion of third body adhered in the disc surface is often called tribofilm. The tribofilm plays an important role in avoiding direct contact between the BFM with the disc [10], contributing to stabilize the friction [11] and to reduce the tribopair wear [12]. The tribofilm is basically formed by iron oxide in the form of magnetite [13–15], mixed with some BFM constituents [16]. On the other hand, the portion of third body clustered around the metallic fibers (primary contact plateaus) of the BFM is assigned to form the secondary contact plateaus [17]. Studies have shown that contact plateaus can influence the friction [18], wear [19] and noise [20] during braking applications. Typically, 30% of the nominal area of the BFM correspond to the primary and secondary contact plateaus, representing the real area of contact [17]. The remaining area is known as lowlands, described as an irregular and rough surface with no contact with the disc [17,21]. The contact plateaus have a relatively long life over braking applications, with slow changes in shape and size [22]. Finally, it is also necessary to consider that a portion of the wear debris is released from the tribopair into the environment. Nowadays, it is an important issue and cannot be neglected since these released wear debris could harm the environment [23].

Recent studies [9,24] have addressed the transition in the wear regime for friction materials applied in automotive brakes. According to those studies, high contact pressures and high sliding velocities have an important influence on the third body, leading to the destruction of the contact plateaus on the BFM, as well as to a removal of the tribofilm on the disc's surface. Then, a sudden increase in friction occurs, and a high wear rate of the BFM was reported. However, these studies did not characterize the composition of the third body (tribofilm and contact plateaus), nor the wear debris released from the tribological interface in the moderate and severe wear regimes. Besides, a detailed explanation of the sequence of events that results in the transition of the wear regime was also missing in those literatures. The elucidation of the wear regime transition sequence, as well as the understanding about the role of the tribofilm in braking applications, are the novelties in the present paper. Those are fundamental factors to be considered by BFM's manufactures for the development of new formulations. For instance, as will be described in this work, it was found that the destruction of the contact plateaus in high contact pressures occurs since they are not able to support high tensile strength. This process was related to the severe wear regime. Considering the above-mentioned research gaps and issues, the present article is dedicated to provides a complete description of the cause-effect events in the transition of the wear regimes of BFM. An extensive experimental work was performed in order to offer a comprehensive characterization of the third body (tribofilm and contact plateaus) and released wear debris in moderate and severe wear regimes. Special techniques, such as Scanning Electron Microscope (SEM), Energy-Dispersive X-ray Spectroscopy (EDX) and Raman Spectroscopy were employed aiming to provide an in-depth overview of the pad-disc contact during different wear regimes.

2 Methodology

2.1 Materials

A commercial brake friction material was used in the tests carried out in the present study. Samples with a cylindrical shape (diameter of 15 mm) were obtained from those brake pads. These samples were rubbed against a grey cast iron disc (diameter of 159 mm) during the braking tests. The approximate composition of the friction material is shown in Table 1.

Table 1
Approximate composition of the friction material used in the experiments.

Category		Volume fraction [%]
Fiber	Metallic	20
	Non-metallic	2
Binder	Phenolic resin	20
	Viscoelastic	10
Lubricants		28
Abrasives		5
Filler		15

Table 2 shows some mechanical properties of the friction material utilized in the present study. Young's modulus and maximum shear stress are obtained through standard ISO6311[25], and the density was calculated based on Standard NBR5544 [26].

Table 2
Mechanical properties of the friction material.

Properties	Standards	Value	Accuracy
Young's modulus [MPa]	ISO6311	535.40	0.33 MPa
Maximum shear stress [MPa]	ISO6311	19.54	0.33 MPa
Density [g/cm³]	NBR5544	2.94	4.04%

2.2 Test apparatus and setup of the experiments

The tests were conducted in a laboratory-scale tribometer with a pin-on-disc configuration, which replicates the operating parameters (sliding velocity, contact pressure and temperature) existent in vehicles' brake systems. During the tests, this device continuously calculates the coefficient of friction (μ) and monitors the temperature through a k-type thermocouple embedded inside the brake disc. More details about this tribotester can be found in [27], [28] and [29].

Two sets of braking parameters were used in the present study. Each of these sets of parameters was performed to reach a different wear regime, i.e., moderate or severe. These parameters were also previously employed in [14]. To reach the moderate wear regime, the braking test was performed with a sliding velocity of 4 m/s and a contact pressure of 2.5 MPa. On the other hand, to reach the severe wear regime the sliding velocity remained the same (4 m/s), and the contact pressure was elevated to 4.5 MPa.

Each test consists of three distinct sections. The first one, named conditioning section, was based on the AK Master test procedure SAE J2522 [30]. In this procedure, a wide range of contact pressure, sliding velocity and initial temperature of the disc is applied through several braking applications. The conditioning section aimed at conforming the surface of the brake friction material on the disc's surface, thereby stabilizing friction. So, the results of the conditioning section will not be discussed in the present paper. The stabilization section consisted of 200 braking applications to ensure that the wear regime (moderate or severe) was well established. Finally, the last section was the debris collection. In this section, an apparatus was used to collect the debris released from the tribological interface during the braking applications. Details about this apparatus will be discussed later (chapter 2.4). The test parameters of the debris collection section were the same of the stabilization section, as shown in Table 3. All the braking applications of the stabilization and debris collection section were performed in drag mode (constant sliding speed of 4 m/s and duration of 7.5 s), and had an initial disc temperature of 100°C.

Table 3. Setup of the tests.

Section	Braking application	Sliding velocity [m/s]	Contact pressure [MPa]	Duration [s]	Initial temperature of the disc [°C]
Conditioning	100	Based on AK Master procedure (SAE J2522)			
Stabilization	200	4	2.5 / 4.5	7.5	100
Debris collection	10				

2.3 Wear measurements

An electronic balance (Marte, model AY 220), with precision of ± 0.1 mg, was used to measure the wear of the samples in the experiments. The samples' mass variation was registered after 200 and 10 braking applications for the stabilization and debris collection sections, respectively. Then, the mass variation was normalized by the summation of the total braking energy obtained for each section. The braking energy of a single braking application is given by the product of the friction force and the sliding distance. Thus, the normalized wear for each section is given by Equation (1) [9]:

$$\Delta W_N = \frac{1000 \cdot \Delta_m}{\sum F_N \bar{\mu} d} \quad (1)$$

where ΔW_N is the normalized wear [mg/J], Δ_m is the sample mass variation [g], F_N is the normal force applied by the sample (pin) [N], $\bar{\mu}$ is the average friction for an individual braking application [-] and d is the sliding distance of a single braking application [m].

2.4 Debris collector apparatus

In order to allow the debris collection during braking applications in the debris collection section, an apparatus was developed and integrated in the laboratory-scale tribometer. This apparatus consists of a metallic collector, a filter and a vacuum air system. The collector is connected to the machine's frame, covering half of the disc. The debris released from the contact are then forced to pass through the filter, which is attached to a filter holder. Then, this filter is extracted from the holder, allowing the analysis of the debris through a microscope. A similar methodology to evaluate the debris was performed by Gehlen et al. [3]. Figure 1 shows the apparatus used to the debris collection.

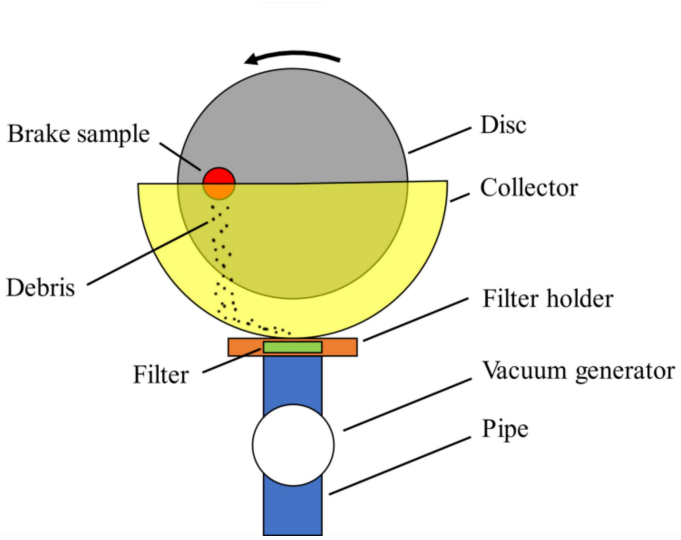

Figure 1. Debris collector apparatus.

2.5 Brake samples, disc and debris characterization

A thermogravimetric analysis (TGA) of the friction material (sample) was performed through a Ta Instrument equipment, model Q50. This technique allows to evaluate the weight variation of the sample as a function of the increase of the temperature. A heating rate of 20°C/min was applied (in air atmosphere).

After the experiments, the surfaces of the discs and samples were measured through an interferometer Bruker, model ContourGT-K. This equipment allows to obtain a tridimensional topography of the surfaces with horizontal and vertical resolution of 4 µm and 0.01 µm, respectively. The scale-limited surfaces for roughness assessment were obtained by robust gaussian filtering with 2.5 mm cut-off. Finally, the roughness of the disc and sample's surfaces were evaluated in terms of the root mean square average (Sq) and skewness (Ssk) roughness parameters according to ISO 25178-2 [31]. A Raman spectroscopy analysis was

carried out to evaluate the kind of oxide formed on the friction track of the discs, as well as on the secondary contact plateaus of the friction materials. A Raman Spectrograph Renishaw, model Invia, utilizing a laser with wavelength of 514 nm was used. Then, the results obtained from the Raman were compared with the literature data.

Micrographs of the sample's worn surfaces were registered through a microscope Zeiss, model Axio Lab. A1. These micrographs were analyzed by a Matlab code, which is based on the Otsu algorithm [32], allowing to estimate the area ratio of contact plateaus. This code was applied in previous studies of the current research group [1,33–35] in order to analyze the contact plateaus of friction materials. A stereoscope Zeiss, model Stemi 508, was also used to analyze the debris obtained during the debris collection section. In addition, the surfaces of the friction materials were also analyzed through a Scanning Electron Microscope (SEM) backscattered electrons mode (Hitachi, model TM3000). Besides, information of the composition of the friction track of the disc was obtained by means of Energy-Dispersive X-ray Spectroscopy (EDX) SWIFT ED 3000.

Finally, after each braking application, a photograph of the disc's surface was automatically captured through a Canon digital camera, model EOS Rebel T6i, equipped with a lens Canon model Ef 100mm F/2.8 Macro USM. The photographs are then analyzed by a Matlab code, which estimates the amount of tribofilm distributed on the disc's surface. This estimation is based on the pixel intensity of the tribofilm observed over the disc's friction track (for each photo). The higher the pixel intensity, the higher the tribofilm deposited on the disc's surface. This technique and method was applied in other studies [9,24] of the current research group.

3 Results and discussion

3.1 TGA

Figure 2 shows the results of TGA of the friction material. This figure also presents the results of the derivative thermogravimetry (DTG). As the temperature rises, the TGA displays the mass degradation, whereas the DTG displays the rate of the degradation process. This curve allows a better visualization of the temperature that occurs the highest weight variation.

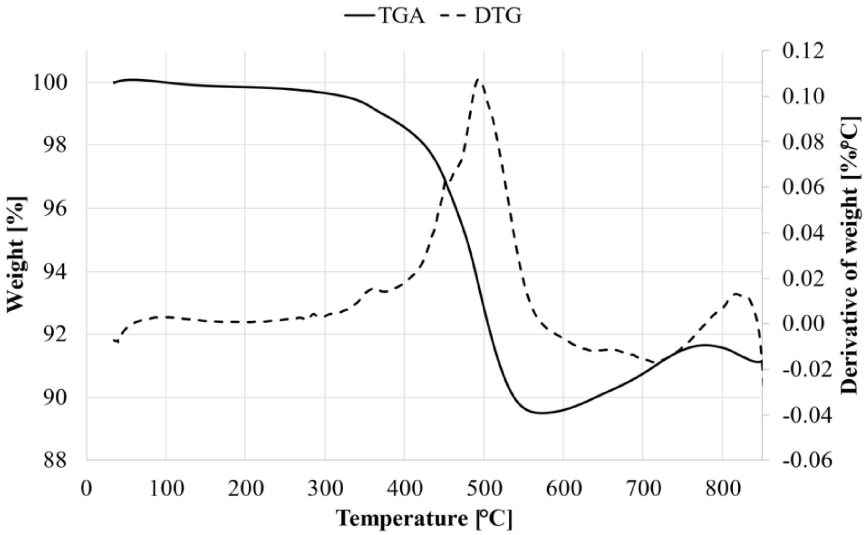

Figure 2. TGA and DTG curves of the friction material in air atmosphere.

It is possible to observe that up to 300°C, a smooth weight reduction of the sample occurs (about 1%). This reduction is due to the water evaporation, as well as the loss of the gas contained in the pores of the brake friction material [36]. A sharp reduction of the weight percentual is observed between 300°C and 600°C. At this range of temperature, the degradation of the phenolic occurs [37]. Since in this analysis the friction material kept a significant portion (~ 90%) of its weight, it is an indicative of a good thermal resistance. An increase in weight is observed around 600°C and above it. According to the literature [36], this increase is a consequence of the oxide formation in the metal particles present in the friction material. In other words, the air atmosphere applied in the TGA contributes to an increase in the weight due to the oxidation of the metal particles.

3.2 Wear, Friction, tribofilm and contact plateaus

Figure 3 shows the normalized wear of the samples obtained in the stabilization and debris collection sections for both tests (high and low contact pressure). The error bars represents the uncertainties for the normalized wear, and were calculated based on [28] and [29].

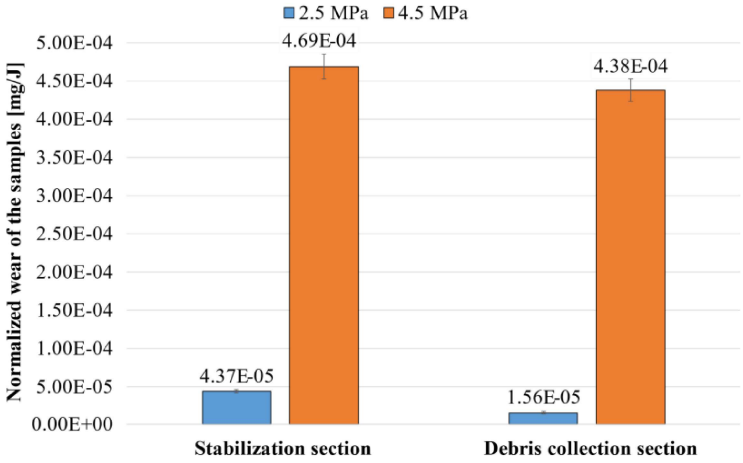

Figure 3. Normalized wear of the samples obtained in the stabilization and debris collection sections.

A significant difference in wear is seen between the experiments with high (4.5 MPa) and low contact pressure (2.5 MPa). In both sections (stabilization and debris collection), wear of the samples was an order of magnitude higher for the experiment with high contact pressure than for the low contact pressure. This confirms that severe wear regime was reached during the high contact pressure experiments.

Friction and tribofilm results are shown in Figure 4. It is worth noticing that the number of braking applications started in 0, since the prior section (conditioning) is not discussed in the present study. Thus, the first braking application shown in Figure 4 refers to the first braking performed in the stabilization section.

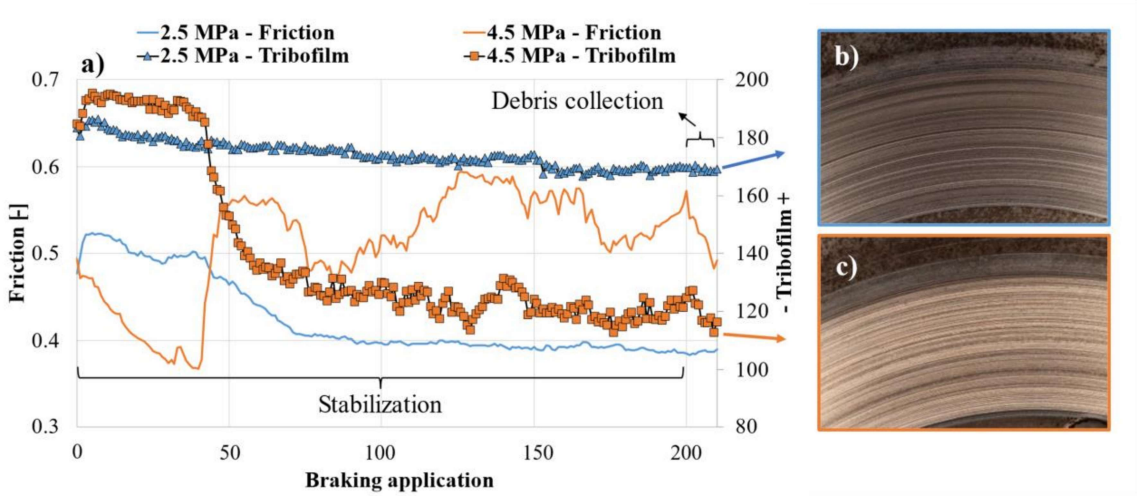

Figure 4. Results of the experiments: (a) friction curves and tribofilm analysis obtained in the stabilization and debris collection sections, image of the disc's surface after (b) low pressure (2.5 MPa), and (c) high pressure (4.5 MPa) tests.

In the experiment with contact pressure of 2.5 MPa (related to the moderate wear regime), it is observed a friction relatively high ($\mu \sim 0.50$) until the braking 41. After that, a slow reduction in friction occurs, followed by a stabilization around to $\mu = 0{,}39$ until the end of the experiment. On the other hand, the tribofilm deposited on the disc's surface showed a smooth decrease, followed by a stable behavior from braking 153 and beyond. Figure 4-b shows the final aspect of the disc surface in the low contact pressure, where it is possible to observe a relatively high deposit of tribofilm.

For the experiment performed under high contact pressure (4.5 MPa - severe wear regime), a distinct behavior occurs when compared with the experiment at 2.5 MPa. Then, a sudden increase in the friction occurs, from 0.37 (braking 37) to 0.56 (braking 54), with an abrupt reduction in tribofilm amount distributed on the disc's surface. This indicates (as well as the results of wear, presented in Figure 3) a transition in wear regime from moderate to severe. After that, substantial variations of friction occur. Figure 4-c shows the final aspect of the disc's surface for the experiment performed under high contact pressure (4.5 MPa). After the severe wear regime (4.5 MPa), the disc's surface appears brighter, indicating that the tribofilm deposited on the disc's surface was removed. On the other hand, a high deposit of tribofilm was observed after the experiment performed under low contact pressure (2.5 MPa). The same results were observed in experiments performed in [9], indicating that the present study reproduce the moderate and severe wear regimes successfully.

The surface of the samples produced by both experiments (high and low contact pressure) is shown in Figure 5.

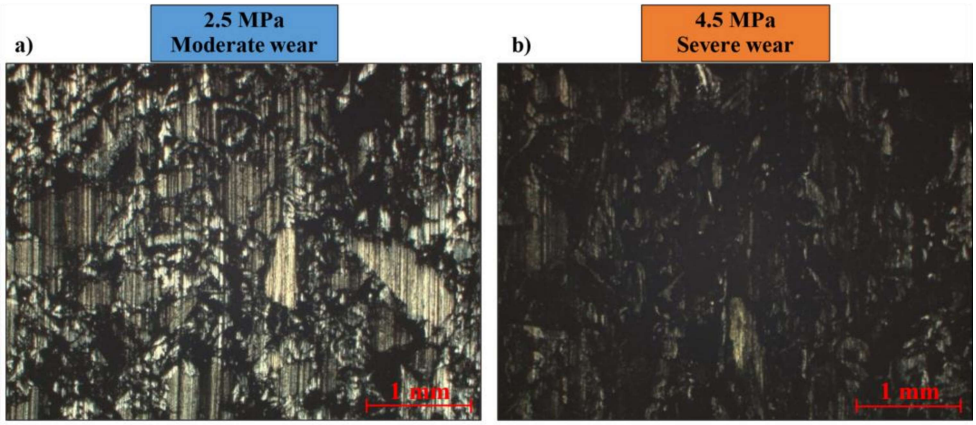

Figure 5. Microscopy of the sample's worn surface after the experiments performed at (a) 2.5 MPa, and (b) 4.5 MPa.

From Figure 5, a clear difference between the surfaces is seen. In the experiment performed under low contact pressure (2.5 MPa), large and visible contact plateaus are formed on the sample's surface (Figure 5-a). On the other hand, for the experiment performed under high contact pressure (4.5 MPa), few contact plateaus are seen on the sample's surface (Figure 5-b). The Otsu algorithm of these microscopies resulted in an area ratio of contact plateaus of 17.23% and 6.23% for 2.5 MPa and 4.5 MPa, respectively. In other words, the experiment with higher contact pressure provided an area ratio of contact plateaus almost 3 times lower than the experiment with 2.5 MPa. The same behavior is reported by [24] and [9], indicating that the severe wear regime occurs in experiment with pressure of 4.5 MPa. Figure 6 exhibits SEM images of the sample's surface for both experiments.

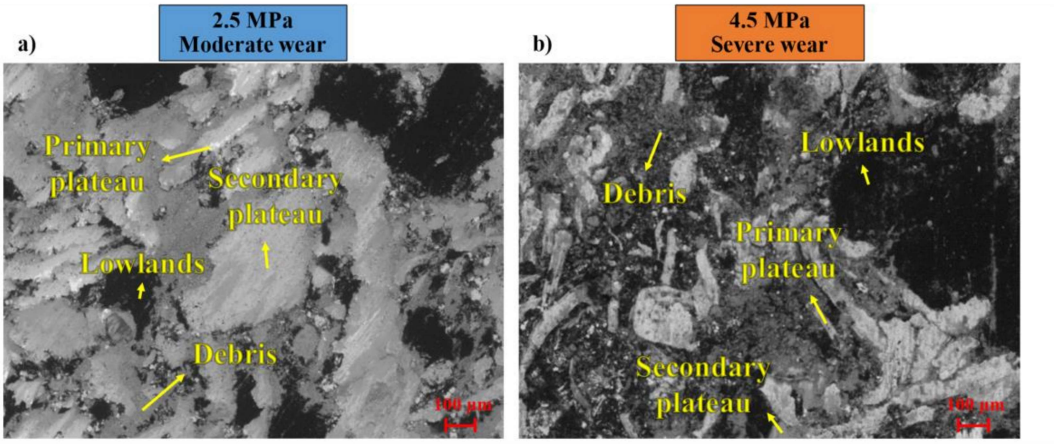

Figure 6. SEM images of the worn surfaces of the friction materials after the experiments performed at (a) 2.5 MPa, and (b) 4.5 MPa.

It is observed that in moderate wear regime (Figure 6-a), the secondary plateaus are well distributed, covering large areas in the image. Only few and small areas of primary contact plateaus (metallic fibers) are visible. This is due to the fact that the primary plateaus are covered by the secondary plateaus. In case of the severe wear regime (Figure 6-b), SEM image shows that most of the primary contact plateaus are exposed (visible) due to the small number of secondary plateaus. Besides, a high amount of debris on the sample's surface is observed. The high contact pressure prevents accumulation of debris, which in turn avoids the formation of secondary plateaus. It is known from literature [22] that accumulation of large amounts of debris is required to secondary plateaus formation.

3.3 Debris analysis

An analysis of the wear debris collected in the high and low contact pressure tests is complementary and will help towards a better comprehension of the processes that take place in both wear regimes (moderate and severe). The debris collected during the 10 braking applications of the debris collection section are shown in Figure 7.

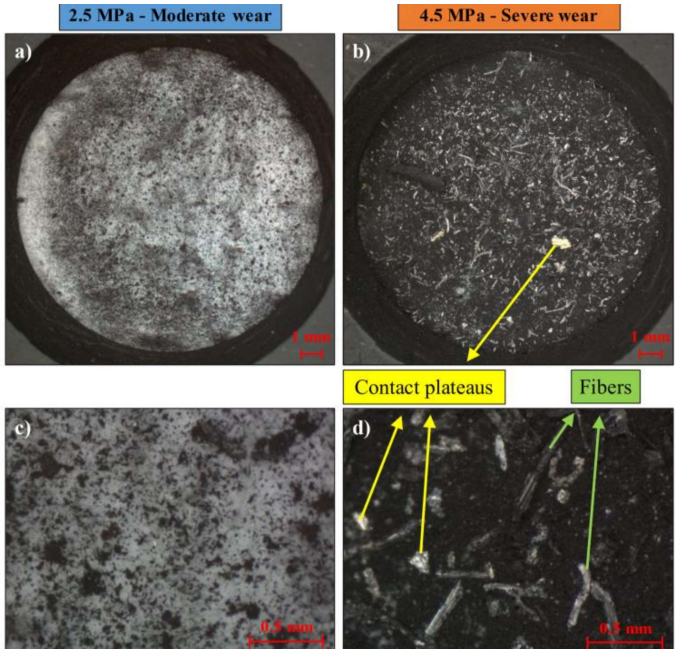

Figure 7. Images of the collected debris, in low magnification (a) 2.5 MPa, and (b) 4.5 MPa, and in high magnification (c) 2.5 MPa and (d) 4.5 MPa.

From Figure 7, it is seen a clear difference between the debris collected at contact pressures of 2.5 MPa and 4.5 MPa. In the moderate wear regime (2.5 MPa, Figure 7-a), fewer amounts of debris were collected, allowing the filter (white paper) to be visible in the background. On the other hand, in the severe wear regime (4.5 MPa, Figure 7-b), the debris covered all the surface of the paper filter. This indicates that a high number of debris was released from the tribological interface. Large metallic fibers (length of ~0.5 mm) are observed in the high contact test (4.5 MPa), suggesting that the severity of the contact was high enough to remove these metallic fibers from the friction material. Besides, large particles are deposited on the filter, as shown in Figure 7-d. These particles seem to be secondary contact plateaus that were removed from the sample's surface. This is an interesting finding, suggesting that in the severe wear regime, the contact plateaus are not stable over the braking applications. They are pulled out from the friction material due to the high contact pressure, resulting in considerable mass loss (i.e., wear).

3.4 Topography and roughness of the brake disc and friction materials

Tridimensional topography of the friction materials obtained after the experiments performed at 2.5 MPa and 4.5 MPa, are shown in Figure 8.

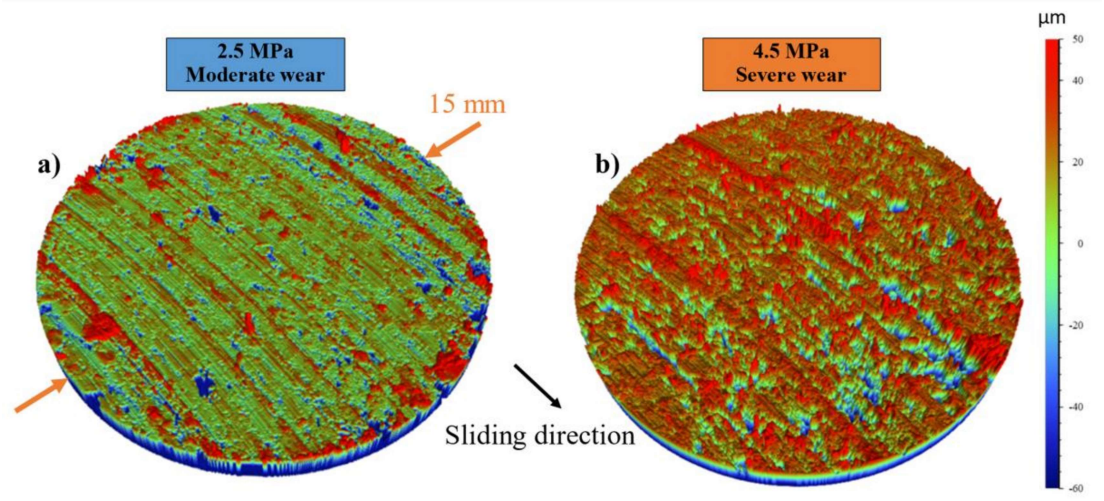

Figure 8. Topography of the sample's surfaces after the experiments carried out at (a) 2.5 MPa, and (b) 4.5 MPa.

For the moderate wear regime (2.5 MPa, Figure 8-a), a relatively flat and smooth surface is observed, with few peaks and valleys. On the other hand, in the severe wear regime (4.5 MPa, Figure 8-b), a more irregular surface is seen. This is due to the high wear rate, which led to deeper scratches marks on the friction material's surface.

Figure 9 exhibits the surface roughness results for both experiments in terms of Sq and Ssk.

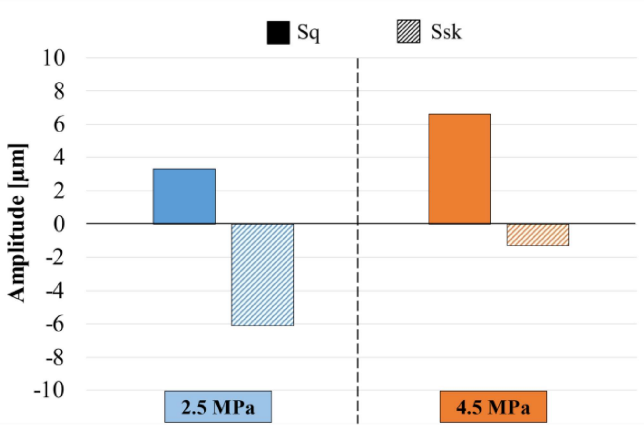

Figure 9. Roughness Sq and Ssk measured on the sample's surface for both experiments.

From Figure 9, it is seen a higher roughness Sq in the severe wear regime (4.5 MPa) than in the moderate wear regime (2.5 MPa). Besides, according to the literature [38], negative values of Ssk indicates a surface with higher quantity of valleys than peaks, and positive values of Ssk reflects the opposite (more peaks than valleys). Thus, a more negative Ssk occurred in the moderate wear regime (2.5 MPa), i.e., the surface is skewed towards the valleys. This behavior indicates that the larger primary and secondary plateaus (on the surface of the sample) formed large flat areas on the sample's surface, with fewer peaks. On the other hand, in the severe wear regime, the greater removal of the primary and secondary contact plateaus led to an irregular surface topography, evenly distributed between peaks and valleys, and therefore resulting in Ssk value close to zero.

Figure 10 shows the tridimensional (3D) topography of the discs after the experiments of moderate and severe wear regimes. For both cases, an area 15 mm × 10 mm was selected. It is worth noticing that the width of 15 mm matches with the diameter of the sample (pins of 15 mm in diameter).

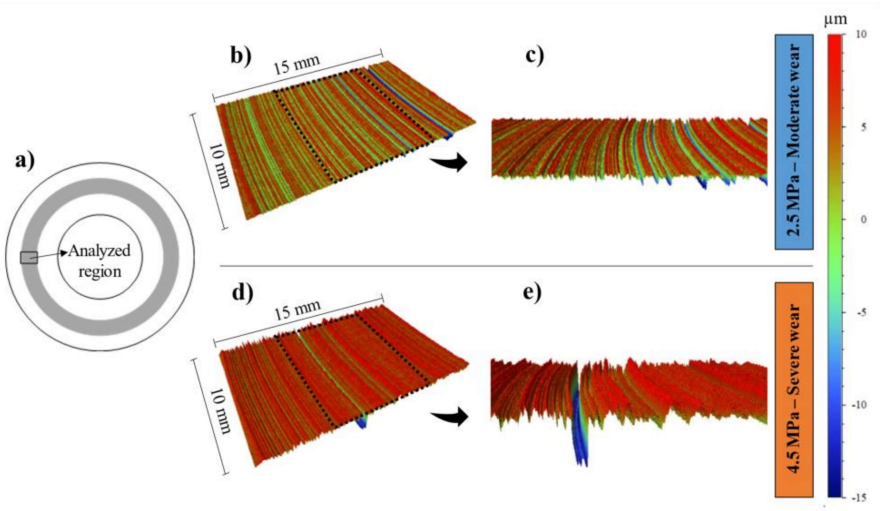

Figure 10. Topography of the disc's surface after the braking test procedure: (a) analyzed region, (b) topography resulting in the low contact pressure (2.5 MPa) experiment, (c) detail of the respective image (2.5 MPa experiment), (d) topography resulting in the high contact pressure (4.5 MPa) experiment, and (e) detail of the respective image (4.5 MPa experiment).

From Figure 10, considering the moderate wear regime, it is observed a relatively homogeneous aspect of disc's surface, indicating a low wear rate of the rotor after the experiments. A distinct behavior occurred in the severe wear regime (Figure 10-d), where deeper scratches are seen in the center of the friction track, indicating the disc underwent a more severe wear rate in case of the 4.5 MPa experiment. Those deeper marks occurred due to a direct contact of the metallic fibers of the friction material with the metal disc, since both the tribofilm and the contact plateaus were removed (or pulled out) from the disc and friction material, respectively. So, there was none "third body" to prevent direct contact between the pad and disc. An important finding that can be noticed is that the severe wear regime affects not just the friction material, but the disc as well.

The surface roughness parameters Sq and Ssk obtained for the worn surface of the discs are presented in Figure 11.

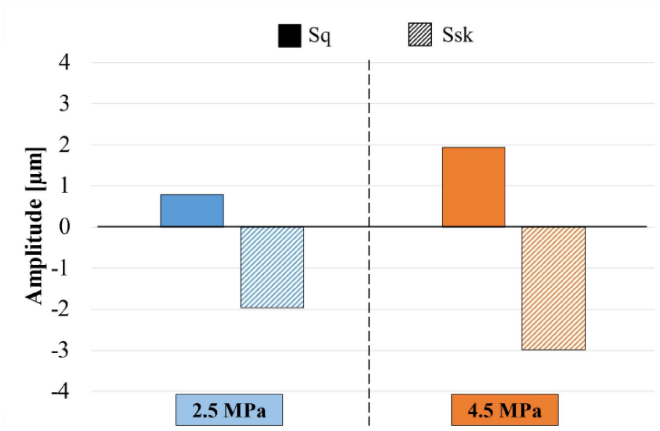

Figure 11. Roughness Sq and Ssk obtained for the friction track surface of the discs for both experiments.

For the experiment performed with high contact pressure (4.5 MPa), a higher value of Sq is noticed when compared with the moderate wear regime, suggesting the disc surface has higher peaks and/or deeper valleys in the severe wear regime. Regarding skewness (Ssk), in both the moderate and severe wear regimes, the discs' surfaces exhibited negative Ssk. However, a more negative value of Ssk was seen in case the high contact pressure experiment (4.5 MPa). This result suggests that the increase in the roughness (indicated by Sq) occurs asymmetrically, in the valley direction, indicating the occurrence of a more severe abrasive wear in the disc. This means that occurred an increase in the valleys' amount and/or valleys depth when the disc underwent the high contact pressure (4.5 MPa) experiment. So, it is concluded that the lower number of secondary plateaus in the severe wear regime, combined with the absence of tribofilm on the disc's surface in this case resulted in higher wear rate for both the friction materials and the brake discs.

3.5 Composition of the worn surfaces

In order to evaluate the kind of oxide formed for both wear regimes, a composition analysis of the worn surfaces (discs and brake materials) is provided. Results of the Raman spectroscopy performed for both worn surfaces is shown in Figure 12. In case of the brake materials, secondary plateaus were selected for this analysis since they are responsible for supporting a significant proportion of the load when the brakes area applied [17].

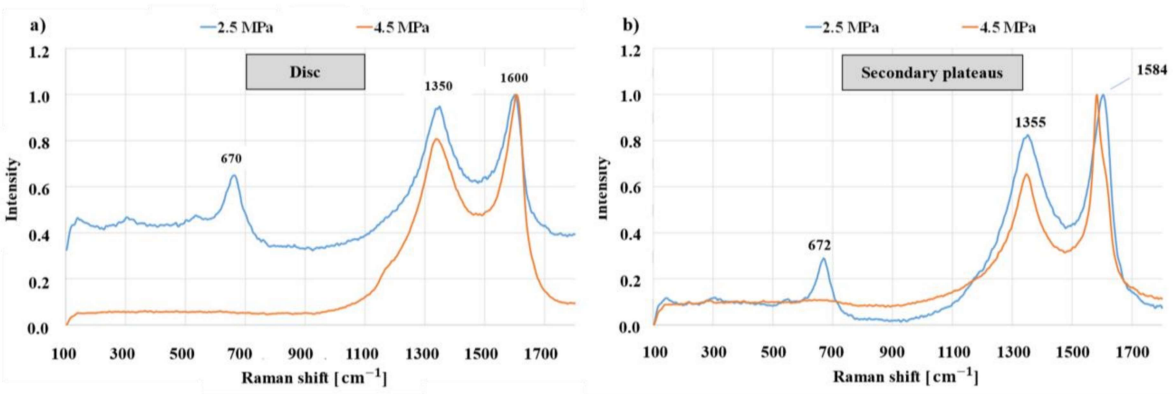

Figure 12. Raman spectroscopy: (a) friction track of the disc, and (b) secondary plateaus after the braking test procedure.

Regarding the friction track of the disc (Figure 12-a), for both experiments, the presence of peaks are seen for 1350 cm^{-1} and 1600 cm^{-1}. According to the literature [39], these peaks are called as D and G bands, respectively, and refer to the presence of carbon. Other authors also found these peaks in the Raman spectroscopy for surfaces of discs rubbed with friction materials [40–42]. A peak in intensity for 670 cm^{-1} was also noticed for the moderate wear regime (2.5 MPa). This peak refers to the formation of iron oxide in the form of magnetite (Fe_3O_4) [43]. The magnetite is described as the main component of tribofilm [13–15], which is known for acting as a friction stabilizer [44]. On the other hand, this peak of magnetite was not observed for the experiment in the severe wear regime (4.5 MPa), indicating that the tribofilm was removed in this regime, as previously discussed. Thus, the absence of magnetite on the disc's surface observed in the experiment performed with high contact pressure seems to explain the high variation in friction observed during the severe wear regime, as previously shown in Figure 4.

A close result was also observed with respect to the surface of the friction materials (Figure 12-b), where peaks around 1350 cm^{-1} and 1600 cm^{-1} are seen for both experiments (2.5 MPa and 4.5 MPa). Besides, a peak in 672 cm^{-1} was observed for moderate wear regime (2.5 MPa), corresponding to the presence of magnetite. Since the secondary plateaus on the friction

material's surface presented a Raman shift behavior like the one observed for the disc (Figure 12-a), the conclusion is that both worn surfaces (disc and friction material) have approximate the same composition. Regarding the severe wear regime (4.5 MPa), the magnetite formation was not detected.

Table 4 shows the results of EDX of the disc, where the chemical composition of the friction track is presented.

Table 4. Chemical composition of the friction track of the disc.

	% in weight	
Element	**2.5 MPa Moderate wear**	**4.5 MPa Severe wear**
Iron	77.4	98.6
Oxygen	19.7	-
Sulfur	2.0	-
Silicon	0.9	1.4

It is possible to observe that for the experiment performed in the moderate wear regime, iron and oxygen were detected, with some amount of sulfur and silicon. The higher content of iron and oxygen indicates the presence of tribofilm on the disc's surface for this experiment, since the tribofilm is mainly formed by iron oxide and elements presented in the friction material [16]. On the other hand, for the experiment performed in the severe wear regime, a higher concentration of iron was also detected through EDX. However, oxygen was no longer observed on the disc's surface for this case. It indicates that a considerable reduction of the tribofilm on the disc occurred in the severe wear regime.

3.6 Discussion

The experiments performed in this study have shown distinct behaviors in moderate and severe wear regimes. For the moderate wear regime, a relatively low and stable friction was observed, with the formation of relatively large contact plateaus on the surface of the friction materials, as well as a developed tribofilm on the disc's surface. This tribofilm was stable during the braking applications performed in the experiment with low contact pressure, as presented in Figure 4. On the other hand, for the experiment performed with high contact pressure (4.5 MPa), a higher and more instable friction occurred, with a low amount of tribofilm on the disc's surface. Besides, a low amount of contact plateaus was formed, indicating that they are not stable in brakings performed under high contact pressures.

According to Eriksson and Jacobson, 2000 [17], the secondary contact plateaus have a high compressive strength, and a low tensile strength. Thus, it is important to evaluate how is the stress field in the secondary plateaus for both experiments. Figure 13 shows a model for the plane stress field of a secondary plateaus during a braking application.

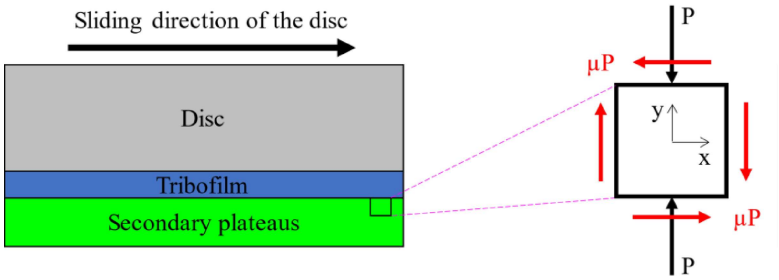

Figure 13. Plan stress field of the secondary plateaus.

Considering the model of the Figure 13, the applied contact pressure (P) induces a friction between the contact materials (disc and pad). Thus, the friction force leads to a shear stress τ, given by the product of friction and pressure ($\tau = \mu P$) [45]. Based on Mohr's circle and assuming the mean friction obtained in the debris collection section (average of 10 braking applications), it is possible to calculate the principal stresses (σ_1 and σ_2), given by Equation (2) and Equation (3).

$$\sigma_1 = -\frac{P}{2} + \sqrt{\left(\frac{P}{2}\right)^2 + (-P\bar{\mu})^2} \tag{2}$$

$$\sigma_2 = -\frac{P}{2} - \sqrt{\left(\frac{P}{2}\right)^2 + (-P\bar{\mu})^2} \tag{3}$$

where σ_1 is the maximum principal stress [MPa], σ_2 is the minimum principal stress [MPa], P is the contact pressure applied in the experiments [MPa], and $\bar{\mu}$ is the mean friction obtained for the debris collection section [-]. Besides, the maximum shear stress [MPa] (τ_{Max}) is given by Equation (4).

$$\tau_{Max} = \sqrt{\left(\frac{P}{2}\right)^2 + (-P\bar{\mu})^2} \quad (4)$$

Finally, the maximum shear stress angle [°] (θ) is given by Equation (5).

$$\theta = \frac{1}{2}\arctan\left(\frac{1}{2\bar{\mu}}\right) \quad (5)$$

Table 5 summarize the values of σ_1, σ_2, τ_{Max} and θ for both experiments calculated through equations (2), (3), (4) and (5), respectively, based on the mean friction of the debris collection section.

Table 5. Mohr's circle results obtained for the model proposed.

Variable	Unit	Moderate wear	Severe wear
P	MPa	-2.5	-4.5
$\bar{\mu}$	-	0.39	0.52
σ_1	MPa	0.34	1.00
σ_2	MPa	-2.84	-5.50
$\tau_{máx}$	MPa	1.59	3.25
θ	°	26.02	21.94

Based on the results presented in Table 5, it is possible to plot the Moh'r circle, presented in Figure 14.

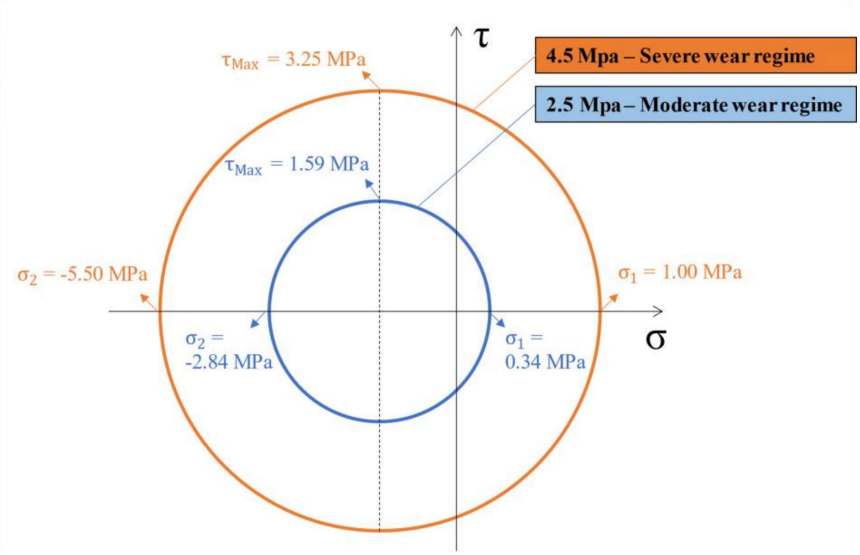

Figure 14. Representation of the Mohr's circle for both experiments.

In the severe wear regime, a higher tensile strength (σ_1 = 1.00 MPa) is observed when compared with moderate wear regime (σ_1 = 0.34 MPa). It occurs due to the high contact pressure (4.5 MPa), which results in a high level of friction. As previously mentioned, the secondary contact plateaus do not support high tensile strength, and then, they are ruined and removed from the friction material's surface. This behavior indicates that there is a critical tensile strength which leads to the destruction of the secondary contact plateaus. As previously reported by [24], the area ratio of contact plateaus is the first parameter that is changed with the increase in contact pressure, leading to the transition in wear regime from moderate to severe. It is worth noting that friction was instable for the severe wear regime, showing the highest magnitude of 0.59 (Figure 4-a).

The actual contact area was reduced with the reduction of secondary contact plateaus in the severe wear regime, and the contact was limited to the primary contact plateaus (metallic fibers). Then, a higher local contact pressure was established between the metallic fibers and the tribofilm deposited on the disc's surface. This "severe" contact led to a gradual removal of the tribofilm as the braking applications proceed, resulting in a direct contact between the metallic fibers and the metal disc. Thus, a higher wear rate occurs for the discs, with deep scratch marks seen on their surfaces, as shown in Figure 10-e. Besides, the increase in the friction materials wear occurs due to the fact that there were no stable contact plateaus during the braking applications. The sequence of events of the transition in wear regime from moderate to severe is illustrated in Figure 15.

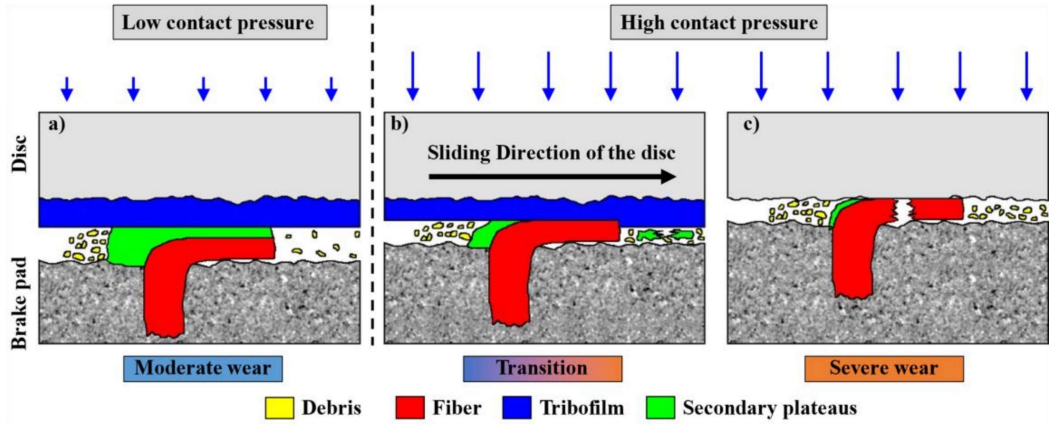

Figure 15. Sequence of events: (a) moderate wear, (b) transition, and (c) severe wear regime.

Literature reports that in the tribological contact of a pad-disc system, plastic deformation of the metallic fibers of brake pads occurs [46,47]. In a condition of moderate wear regime (Figure 15-a), a well-developed tribofilm is established, and relatively large secondary plateaus are formed by the accumulation of debris. Those mechanisms (tribofilm plus contact plateaus) prevent direct contact between the fiber (primary contact plateaus) and the metal disc. Some debris are released from the tribological interface, as previously seen by the collected debris in Figure 7-a. With a higher contact pressure (e.g., 4.5 MPa), the secondary contact plateaus are not able to support the load due to the high tensile strength (Figure 15-b). So, they break and release from the friction material, as proved by the large particles collected in severe wear regime (Figure 7-b). Besides, the high load prevents the debris accumulation, which is required to form the secondary contact plateaus. The absence of secondary plateaus stabilizes higher friction values, which leads to a state of stress on the contact surface with higher tensile and shear stresses, making it difficult to rebuild secondary plateaus. Besides, the lack of secondary plateaus results in a direct contact between metallic fibers of the friction material and the disc's tribofilm, leading to the removal of the latter (tribofilm) over the braking applications (Figure 15-b). The absence of tribofilm results in a more severe abrasive wear on the disc's surface due the contact between the metallic fibers and the metal disc (Figure 15-c), resulting in a high and instable friction. Occasionally, this contact leads to the rupture of the metallic fibers, as previously shown in Figure 7-d.

The secondary contact plateaus and the tribofilm have a fundamental role in the transition of the wear regime. Brake friction materials capable of forming stable secondary contact plateaus, along a well-developed tribofilm on the disc in a wide range of brake conditions leads to a tribopair with lower wear rate. Thus, both mechanisms (secondary plateaus and tribofilm formation) are fundamental aspects to be considered in order to have a friction material with stable friction and low wear rate.

4 Conclusions

The present study focused on the characterization of the third body deposited on the disc's surface (tribofilm) and on the brake friction material (contact plateaus). Besides, an explanation of the sequence of events that occurs in the transition in wear regime from moderate to severe is presented. The main findings are listed below:

- The severe wear regime affects not just the friction material, but also the disc, where deep scratches were observed on its surface.
- Iron oxide in the form of magnetite (Fe_3O_4) was observed on the tribofilm and on the secondary contact plateaus in the moderate wear regime. On the other hand, in the severe wear regime, the magnetite was not identified, resulting in a high variation in friction observed in this regime.
- Large particles (metallic fibers and secondary plateaus) were collected during the braking applications performed under high contact pressure. This behavior indicates that secondary plateaus are not stable in this condition.
- There is a critical tensile strength which leads to the destruction of the secondary contact plateaus and makes their reconstitution difficult. This behavior can be explained through the Mohr's circle, where the high contact pressure applied in the experiments exceeded the maximum tensile strength of the contact plateaus.
- The destruction of the secondary contact plateaus leads to a direct contact between metallic fibers of the friction material and the disc's tribofilm. Thus, the tribofilm is removed over the braking applications. The absence of tribofilm results in a more severe abrasive wear on the disc's surface, as well as it increased the wear rate of BFM.

This study significantly advanced the current knowledge on wear phenomena in brake systems. In this paper, it was shown that the transition from moderate to severe regime underwent significant changes, not only in the traditional indicators of tribological applications (wear and friction), but also in the topography, morphology and chemical composition of the matching surfaces. The insights gained from this research contribute for improving the BFM, where a better understanding of the wear regime transition can be used for the development of durable materials with a stable friction under various operating conditions.

Acknowledgements

The authors are grateful by the support of the Brazilian research agencies CNPq (Conselho Nacional de Desenvolvimento Científico e Tecnológico) and CAPES (Coordenação de Aperfeiçoamento de Pessoal de Nível Superior - Finance Code 001), as well as the Fras-le S/A company. A. Ramalho like to thank the support of FCT – Fundação para a Ciência e a Tecnologia, through national funds under the project UIDB/00285/2020 and LA/P/0112/2020.

References

[1] G.S. Gehlen, P.D. Neis, L.Y. Barros, J.C. Poletto, N.F. Ferreira, S.C. Amico, Tribological performance of eco-friendly friction materials with rice husk, Wear. 500–501 (2022) 204374. https://doi.org/10.1016/j.wear.2022.204374.

[2] H.A. Moghadam, S. Banaeifar, R. Tavangar, A.R. Khavandi, S. Mahdavi, Resin-Based Copper-Free Brake Pads: A Right Selection of Potassium Titanate and Ceramic Fiber, Iran. J. Mater. Sci. Eng. 19 (2022) 1–15. https://doi.org/10.22068/ijmse.2320.

[3] G.S. Gehlen, A.P.G. Nogueira, D. Carlevaris, L.Y. Barros, J.C. Poletto, G. Lasch, G. Straffelini, N.F. Ferreira, P.D. Neis, Tribological assessment of rice husk ash in eco-friendly brake friction materials, Wear. 516–517 (2023) 204613. https://doi.org/10.1016/j.wear.2022.204613.

[4] T. Singh, Comparative performance of barium sulphate and cement by-pass dust on tribological properties of automotive brake friction composites, Alexandria Eng. J. 72 (2023) 339–349. https://doi.org/10.1016/j.aej.2023.04.010.

[5] J. Duan, M. Zhang, P. Chen, Z. Li, L. Pang, P. Xiao, Y. Li, Tribological behavior and applications of carbon fiber reinforced ceramic composites as high-performance frictional materials, Ceram. Int. 47 (2021) 19271–19281. https://doi.org/10.1016/j.ceramint.2021.02.187.

[6] W. Lertwassana, T. Parnklang, P. Mora, C. Jubsilp, S. Rimdusit, High performance aramid pulp/carbon fiber-reinforced polybenzoxazine composites as friction materials, Compos. Part B Eng. 177 (2019) 107280. https://doi.org/10.1016/j.compositesb.2019.107280.

[7] P.J. Blau, Compositions, functions, and testing of friction brake materials and their additives, Oak Ridge Natl. Lab. Tech. Report, ORNL/TM-2001/64 29 Pp. Available through NTIS.gov. (2001) 38. https://doi.org/http://dx.doi.org/10.2172/788356.

[8] G.P. Ostermeyer, L. Wilkening, Experimental investigations of the topography dynamics in brake pads, SAE Int. J. Passeng. Cars - Mech. Syst. 6 (2013). https://doi.org/10.4271/2013-01-2027.

[9] L.Y. Barros, J.C. Poletto, D. Buneder, R. Flores, G. Gehlen, P.D. Neis, N.F. Ferreira, L.T. Matozo, An experimental study of the transition in the wear regime of brake friction materials, Polym. Compos. (2021) 1–12. https://doi.org/10.1002/pc.26299.

[10] H. Jang, K. Ko, S.J. Kim, R.H. Basch, J.W. Fash, The effect of metal fibers on the friction performance of automotive brake friction materials, Wear. 256 (2004) 3–4. https://doi.org/10.1016/S0043-1648(03)00445-9.

[11] a. L. Cristol-Bulthé, Y. Desplanques, G. Degallaix, Coupling between friction physical mechanisms and transient thermal phenomena involved in pad-disc contact during railway braking, Wear. 263 (2007) 1230–1242. https://doi.org/10.1016/j.wear.2006.12.052.

[12] M.G. Jacko, P.H.S. Tsang, S.K. Rhee, Wear debris compaction and friction film formation of polymer composites, Wear. 133 (1989) 23–38. https://doi.org/10.1016/0043-1648(89)90110-5.

[13] W. Österle, I. Urban, Friction layers and friction films on PMC brake pads, Wear. 257 (2004) 215–226. https://doi.org/10.1016/j.wear.2003.12.017.

[14] R. Hinrichs, M. Vasconcellos, M.R. Soares, Magnetite generated by tribo-reactions on the surface of brake pad material, SAE Tech. Pap. (2010). https://doi.org/10.4271/2010-01-1672.

[15] R. Hinrichs, M.A.Z. Vasconcellos, W. Österle, C. Prietzel, A TEM snapshot of magnetite formation in brakes: The role of the disc's cast iron graphite lamellae in third body formation, Wear. 270 (2011) 365–370. https://doi.org/10.1016/j.wear.2010.11.008.

[16] W. Österle, I. Dörfel, C. Prietzel, H. Rooch, a.-L. Cristol-Bulthé, G. Degallaix, Y. Desplanques, A comprehensive microscopic study of third body formation at the interface between a brake pad and brake disc during the final stage of a pin-on-disc test, Wear. 267 (2009) 781–788. https://doi.org/10.1016/j.wear.2008.11.023.

[17] M. Eriksson, S. Jacobson, Tribological surfaces of organic brake pads, Tribol. Int. 33 (2000) 817–827. https://doi.org/10.1016/S0301-679X(00)00127-4.

[18] L.Y. Barros, J.C. Poletto, P.D. Neis, N.F. Ferreira, C.H.S. Pereira, Influence of copper on automotive brake performance, Wear. 426–427 (2019) 741–749. https://doi.org/10.1016/j.wear.2019.01.055.

[19] J. Wahlström, Y. Lyu, V. Matjeka, A. Söderberg, A pin-on-disc tribometer study of disc brake contact pairs with respect to wear and airborne particle emissions, Wear. 384–385 (2017) 124–130. https://doi.org/10.1016/j.wear.2017.05.011.

[20] S.W. Yoon, M.W. Shin, W.G. Lee, H. Jang, Effect of surface contact conditions on the stick-slip behavior of brake friction material, Wear. 294–295 (2012) 305–312. https://doi.org/10.1016/j.wear.2012.07.011.

[21] M. Eriksson, J. Lord, S. Jacobson, Wear and contact conditions of brake pads: Dynamical in situ studies of pads on glass, Wear. 249 (2001) 272–278. https://doi.org/10.1016/S0043-1648(01)00573-7.

[22] M. Eriksson, F. Bergman, S. Jacobson, On the nature of tribological contact in automotive brakes, Wear. 252 (2002) 26–36. https://doi.org/10.1016/S0043-1648(01)00849-3.
[23] J.F. Sandahl, D.H. Baldwin, J.J. Jenkins, N.L. Scholz, A sensory system at the interface between urban stormwater runoff and salmon survival, Environ. Sci. Technol. 41 (2007) 2998–3004. https://doi.org/10.1021/es062287r.
[24] L.Y. Barros, J.C. Poletto, D. Buneder, P.D. Neis, N.F. Ferreira, R.P. Pavlak, L.T. Matozo, Effect of pressure in the transition between moderate and severe wear regimes in brake friction materials, Wear. 438–439 (2019) 203112. https://doi.org/10.1016/j.wear.2019.203112.
[25] ISO, 6311 - Road vehicles - Brake linings - Internal shear strength of lining materials - Test procedure, (1980).
[26] NBR, NBR 5544 - Guarnições da embreagem e do freio - Determinação da densidade relativa, (1998).
[27] P.D. Neis, N.F. Ferreira, F.J. Lorini, Contribution to perform high temperature tests (fading) on a laboratory-scale tribometer, Wear. 271 (2011) 2660–2664. https://doi.org/10.1016/j.wear.2010.12.023.
[28] R.P. Pavlak, P.D. Neis, J.C. Poletto, L.Y. De Barros, N.F. Ferreira, Wear, Friction and NVH Characterization Using a Laboratory-Scale Tribometer, SAE Tech. Pap. Part F1298 (2017) 1–7. https://doi.org/10.4271/2017-36-0003.
[29] P.D. Neis, Projeto e construção de um tribômetro com controle independente da temperatura do disco (in portuguese) [Ph.D. Thesis], Federal University of Rio Grande do Sul (Brazil) and Ghent University, Belgium, 2012.
[30] SAE International, Surface vehicle recommended practice - SAE J2522 - Dynamometer global brake effectiveness (AK Master), 2003.
[31] ISO 25178-2, Geometrical product specifications (GPS) — Surface texture: Areal Part 2: Terms , definitions and surface texture parameters, 2012.
[32] N. Otsu, A Threshold Selection Method from Gray-Level Histograms, IEEE Trans. Syst. Man. Cybern. 9 (1979) 62–66. https://doi.org/10.1109/TSMC.1979.4310076.
[33] D. Masotti, P. Neis, N. Ferreira, K. Gomes, J. Poletto, L. Matozo, Experimental evaluation of surface morphology characteristics during stick-slip process at low speed sliding test, SAE Int. J. Passeng. Cars - Mech. Syst. (2015). https://doi.org/10.4271/2015-01-2685.
[34] P.D. Neis, N.F. Ferreira, J. Sukuraman, P.D. Beats, M. Andó, L.T. Matozo, D. Masotti, Characterization of surface morphology and its correlation with friction performance of brake pads, Sustain. Constr. Des. 6 (2015).
[35] J.C. Poletto, L.Y. Barros, P.D. Neis, N.F. Ferreira, Analysis of the error in the estimation of the morphology of contact plateaus existing on the surface of brake pads, Tribol. Int. 126 (2018) 297–306. https://doi.org/10.1016/j.triboint.2018.05.026.
[36] A.L. Cristol-Bulthé, Y. Desplanques, G. Degallaix, Y. Berthier, Mechanical and chemical investigation of the temperature influence on the tribological mechanisms occurring in OMC/cast iron friction contact, Wear. 264 (2008) 815–825. https://doi.org/10.1016/j.wear.2006.12.080.
[37] R. Yun, P. Filip, Y. Lu, Performance and evaluation of eco-friendly brake friction materials, Tribol. Int. 43 (2010) 2010–2019. https://doi.org/10.1016/j.triboint.2010.05.001.
[38] N. Duboust, H. Ghadbeigi, C. Pinna, S. Ayvar-Soberanis, A. Collis, R. Scaife, K. Kerrigan, An optical method for measuring surface roughness of machined carbon fibre-reinforced plastic composites, J. Compos. Mater. 51 (2016) 289–302. https://doi.org/10.1177/0021998316644849.
[39] A. Dychalska, P. Popielarski, W. Franków, K. Fabisiak, K. Paprocki, M. Szybowicz, Study of CVD diamond layers with amorphous carbon admixture by Raman scattering spectroscopy, Mater. Sci. Pol. 33 (2015) 799–805. https://doi.org/10.1515/msp-2015-0067.
[40] W. Österle, I. Urban, Third body formation on brake pads and rotors, Tribol. Int. 39 (2006) 401–408. https://doi.org/10.1016/j.triboint.2005.04.021.
[41] A.I. Dmitriev, W. Österle, H. Kloß, Numerical simulation of typical contact situations of brake friction materials, Tribol. Int. 41 (2008) 1–8. https://doi.org/10.1016/j.triboint.2007.04.001.
[42] R. Hinrichs, M.A.Z. Vasconcellos, W. Österle, C. Prietzel, Amorphization of Graphite Flakes in Gray Cast Iron Under Tribological Load, Mater. Res. 21 (2018) 2–7. https://doi.org/10.1590/1980-5373-mr-2017-1000.
[43] W. Österle, H. Kloß, I. Urban, A.I. Dmitriev, Towards a better understanding of brake friction materials, Wear. 263 (2007) 1189–1201. https://doi.org/10.1016/j.wear.2006.12.020.
[44] R. Hinrichs, M.R.F. Soares, R.G. Lamb, M.R.F. Soares, M.A.Z. Vasconcellos, Phase characterization of debris generated in brake pad coefficient of friction tests, Wear. 270 (2011) 515–519. https://doi.org/10.1016/j.wear.2011.01.004.
[45] G. Strafellini, Friction and Wear: Methodologies for Design and Control, 2016. http://link.springer.com/10.1007/978-3-662-48465-4.
[46] J. Kukutschová, V. Roubíček, K. Malachová, Z. Pavlíčková, R. Holuša, J. Kubačková, V. Mička, D. MacCrimmon, P. Filip, Wear mechanism in automotive brake materials, wear debris and its potential environmental impact, Wear. 267 (2009) 807–817. https://doi.org/10.1016/j.wear.2009.01.034.
[47] P. Monreal, I. Clavería, P. Arteta, T. Rouzaut, Effect of modified novolac resins on the physical properties and friction performance of railway brake blocks, Tribol. Int. 154 (2021) 106722. https://doi.org/10.1016/j.triboint.2020.106722.